Modeling two-phase ferroelectric composites by sequential laminates



2014 Modelling Simul. Mater. Sci. Eng. 22 025010

(http://iopscience.iop.org/0965-0393/22/2/025010)

IOP Publishing Modelling and Simulation in Materials Science and Engineering

Modelling Simul. Mater. Sci. Eng. **22** (2014) 025010 (20pp) doi:10.1088/0965-0393/22/2/025010

# Modeling two-phase ferroelectric composites by sequential laminates

**Martín I Idiart**

Departamento de Aeronáutica, Facultad de Ingeniería, Universidad Nacional de La Plata, Avda. 1 esq. 47 S/N, La Plata B1900TAG, Argentina
Consejo Nacional de Investigaciones Científicas y Técnicas (CONICET), CCT La Plata, Calle 8 N° 1467, La Plata B1904CMC, Argentina

E-mail: martin.idiart@ing.unlp.edu.ar

Received 9 October 2013
Accepted for publication 10 December 2013
Published 17 January 2014

**Abstract**

Theoretical estimates are given for the overall dissipative response of two-phase ferroelectric composites with complex particulate microstructures under arbitrary loading histories. The ferroelectric behavior of the constituent phases is described via a stored energy density and a dissipation potential in accordance with the theory of generalized standard materials. An implicit time-discretization scheme is used to generate a variational representation of the overall response in terms of a single incremental potential. Estimates are then generated by constructing sequentially laminated microgeometries of particulate type whose overall incremental potential can be computed exactly. Because they are realizable, by construction, these estimates are guaranteed to conform with any material constraints, to satisfy all pertinent bounds and to exhibit the required convexity properties with no duality gap. Predictions for representative composite and porous systems are reported and discussed in the light of existing experimental data.

Keywords: ferroelectrics, composites, homogenization methods, hysteresis

(Some figures may appear in colour only in the online journal)

## 1. Introduction

Ferroelectricity refers to the capacity of certain polar dielectrics to sustain a spontaneous electrical polarization that can be altered by application of an external electric field (Lines and Glass 1977). Since this change in polarization is usually accompanied by a mechanical deformation, ferroelectrics are electro-deformable materials which find applications as sensors

and actuators (e.g. Xu (1991), Capsal *et al* (2012)), energy harvesters (e.g. van den Ende *et al* 2012), material damping enhancers (e.g. Asare *et al* 2012) and other microdevices. Ferroelectric ceramics such as barium titanate and lead zirconate titanate are probably the most prominent examples among this class of materials.

The search for electro-deformable materials with specific combinations of properties not found in monolithic ferroelectrics has recently motivated the development of an increasing variety of two-phase ferroelectric composites. Composites with different purposes have been produced, for instance, by dispersing ferroelectric ceramic particles in a nonpolar polymeric matrix (e.g. Lam *et al* 2005, Capsal *et al* 2012, Olmos *et al* 2012), by dispersing metallic particles in a ferroelectric ceramic matrix (e.g. Duan *et al* 2000, Zhang *et al* 2010, Ning *et al* 2012) and by dispersing ferroelectric ceramic inclusions in a ferroelectric polymeric matrix (e.g. Mao *et al* 2010, Petchsuk 2011). Ferroelectric ceramics with controlled porosity have also been produced for certain acoustic applications (e.g. Piazza *et al* 2010). Now, under sufficiently high electric fields, all these composites exhibit significant electrical hysteresis and dissipation. The main contribution to that overall dissipation comes from the change of spontaneous polarization in the ferroelectric phase—which is the result of certain irreversible processes occuring at the atomic scale (e.g. Damjanovic 2006)—, and its precise amount depends on the dielectric response of each of the constituents and their geometrical arrangement. The purpose of this work is to theoretically estimate such dependence.

The problem calls for a methodology to estimate the overall response of two-phase dielectric composites with complex microstructures and with constituent phases that can simultaneously store and dissipate electrostatic energy. While full-field simulations are certainly an option, the focus here is on semi-analytical estimates requiring low computational power. Following Bassiouny *et al* (1988), we treat the spontaneous—or irreversible—polarization as an internal state variable and describe its evolution via the formalism of generalized standard materials (GSMs). There are several methods already available to homogenize multi-phase GSMs, mostly derived in the context of elasto-viscoplasticity. One of the first rational approaches in that context is due to Hill (1965), who proposed a rate version of the linear self-consistent approximation to improve on the elementary approximations of Taylor (1938) and Sachs (1928). This work spawned a large number of ad hoc linearization schemes which were applied to diverse material systems such as polycrystalline materials and reinforced solids, and it even inspired micromechanical models for polycrystalline ferroelectrics (Huber *et al* 1999). Unfortunately, the estimates produced by these simple methods become inaccurate when the material system exhibits strong constitutive nonlinearities and large heterogeneity contrasts (see, for instance, Chaboche *et al* 2005 and references therein). The main obstacle to deriving accurate estimates for this class of materials was probably the lack of a suitable variational representation of the overall response. Such representation was given a few years ago by Miehe (2002) building on previous work by Ortiz and Stainier (1999). In this incremental variational representation, the field equations are discretized in time in such a way that the constitutive relations can be expressed in terms of a single incremental potential in line with standard variational formulations for purely energetic—or purely dissipative—solids. This fact lead Lahellec and Suquet (2004, 2007a, 2007b) to realize that rigorous estimates could be derived by making judicious use of linear-comparison techniques akin to well-established techniques for purely energetic solids. This promising strategy paved the way for generating a multitude of approximations whose accuracy is progressively being assessed (Lahellec and Suquet 2007a, 2007b, 2013, Brassart *et al* 2011).

An alternative strategy consists in the construction of so-called solvable microgeometries. These are special classes of microgeometries that reproduce the essential geometrical features of the actual composite microstructure while at the same time allowing the exact computation

of the overall potential. The main advantage of this strategy over the aforementioned methods is that the resulting predictions are guaranteed to conform with material constraints, to satisfy all pertinent bounds and to exhibit the required convexity with no duality gap. The strategy was initially pursued by Maxwell (1873) to estimate the overall ohmic resistance of stratified media, and it has developed greatly since then for materials with linear responses characterized by a single potential (see, for instance, Milton 2002 and references therein). Central to this approach was the observation by Maxwell (1873) and Bruggeman (1935) that the set of solvable microgeometries could be enlarged by following iterative procedures whereby the constituent phases in a solvable microgeometry are themselves identified with solvable microgeometries at a lower length scale, thus producing hierarchical microgeometries of increasing complexity whose overall potential can be determined iteratively. For instance, Maxwell (1873) constructed particulate composites with an isotropic response by iterating anisotropic laminated microgeometries; the resulting microgeometries are known as sequential laminates. Bruggeman (1935), in turn, constructed particulate composites with arbitrary volume fractions of particles by iterating microgeometries with dilute volume fractions of particles; this approach is known as the differential scheme. These iterative schemes considerably widened the range of microstructures that could be modeled, and proved very useful in estimating the overall response of two-phase linear dielectrics and other linear media characterized by a single potential.

Now, the use of similar iterative schemes in the context of nonlinear GSMs characterized by two potentials has been encumbered by the facts that: (i) the overall response of a nonlinear composite does not exhibit, in general, the same functional dependence on the external fields as the local responses and (ii) the overall response depends, in general, on an infinite number of internal variables[1]. This study reports on a first attempt to use solvable microgeometries to generate relatively simple—yet representative—models for ferroelectric composites in terms of a finite number of internal variables. We begin in section 2 by formulating the problem of a heterogeneous dielectric body whose constituent phases are modeled as generalized standard materials. The overall reponse of the composite system is then defined in section 3 by invoking the notion of representative volume element of Hill (1963). Making use of the variational representation of Miehe (2002), the overall response of sequentially laminated microgeometries is derived in section 4. The choice of this specific class of solvable microgeometries is motivated by recent works on nonlinear GSMs characterized by a single potential, where sequential laminates have been successfully used to model particulate systems such as viscoplastic composites and porous media (e.g. deBotton and Hariton 2002, Idiart 2006, 2008, Danas *et al* 2008a, 2008b) and non-ohmic composite conductors (Hariton and deBotton 2003). Furthermore, a rigorous geometrical characterization of these microgeometries is now available from the work of Idiart and Ponte Castañeda (2013). Finally, sample results are reported and discussed in section 5 and some concluding remarks are given in section 6.

## 2. The composite material model

### *2.1. The material system and field equations*

The material system under study is idealized here as a heterogeneous body occupying a domain $\Omega$ and made up of a continuous matrix containing a uniform dispersion of inclusions. The matrix phase will be identified with the index $r = 1$ while the inclusions will be collectively identified with the index $r = 2$. Each phase occupies a domain $\Omega^{(r)} \subset \Omega$ $(r = 1, 2)$ such that

[1] This conflicts with one of the practical purposes of homogenization procedures, which is to generate a simple description of the overall response in terms of a reduced number of macroscopic variables.

$\Omega = \cup_{r=1}^{2} \Omega^{(r)}$. The domains $\Omega^{(r)}$ can be described by a set of characteristic functions $\chi^{(r)}(\boldsymbol{x})$, which take the value 1 if the position vector $\boldsymbol{x}$ is in $\Omega^{(r)}$ and 0 otherwise.

We restrict attention to isothermal processes produced by electrostatic interactions only. These interactions are represented by a fixed electrostatic potential $\hat{\phi}$ applied via a surface electrode occupying the portion $\partial\Omega_v$ of the body boundary $\partial\Omega$. For simplicity, we disregard the possible presence of free charges within the material and the effects of electromechanical coupling on the ferroelectric response[2]. The governing field equations are then given by—see, for instance, Kovetz (2000)—

$$\nabla \cdot \boldsymbol{D} = 0 \quad \text{and} \quad \boldsymbol{E} = -\nabla\phi \qquad \text{in } \mathbb{R}^3, \tag{1}$$

$$\phi = \hat{\phi} \quad \text{on } \partial\Omega_v \qquad \text{and} \qquad [\boldsymbol{D} \cdot \boldsymbol{n}] = 0 \quad \text{on } \partial\Omega \backslash \partial\Omega_v, \tag{2}$$

with

$$\boldsymbol{D} = \begin{cases} \epsilon_0 \boldsymbol{E} & \text{in } \mathbb{R}^3 \backslash \Omega, \\ \epsilon_0 \boldsymbol{E} + \boldsymbol{P} & \text{in } \Omega. \end{cases} \tag{3}$$

In these expressions, $\phi$ is the electrostatic potential, $\boldsymbol{D}$, $\boldsymbol{E}$ and $\boldsymbol{P}$ are the electric displacement, the electric field and the material polarization, respectively, $[\cdot]$ denotes the jump across $\partial\Omega$, $\boldsymbol{n}$ is the outward normal vector to $\partial\Omega$ and $\epsilon_0$ denotes the electric permittivity of vacuum. Along internal surfaces of discontinuity, the various fields must satisfy the jump conditions

$$[\phi] = 0, \qquad [\boldsymbol{D} \cdot \boldsymbol{n}] = 0, \tag{4}$$

where $\boldsymbol{n}$ denotes the normal vector to the discontinuity surface. In addition, the electrostatic potential must vanish at infinity, i.e. $\phi \to 0$ as $|\boldsymbol{x}| \to \infty$.

The above field equations must be supplemented with constitutive relations describing the dielectric response of each phase. Given our interest on ferroelectric composites, we follow the thermodynamic approach of Bassiouny *et al* (1988) wherein dissipative processes are characterized by an irreversible polarization $\mathbf{p}$ playing the role of an internal variable. This framework is general enough to characterize simple responses such as linear polarizability as well as complex responses such as rate-dependent ferroelectricity—see, for instance, Kamlah (2001) and Miehe and Rosato (2011).

The total energy of the material system and its surroundings is thus written as

$$\mathcal{E} = \int_\Omega E(\boldsymbol{x}, \boldsymbol{P}, \mathbf{p})\, \mathrm{d}V + \int_{\mathbb{R}^3} \frac{1}{2}\epsilon_0 \boldsymbol{E}^2\, \mathrm{d}V, \tag{5}$$

where the first term corresponds to the energy stored in the composite material while the second term is the electrostatic energy associated with the electric field in the entire space. The energy density $E$ is assumed to be convex in $\boldsymbol{P}$ and $\mathbf{p}$; it is also taken to depend explicitly on position due to the heterogeneity of the body. In turn, the dissipation of the system is assumed to be of the form

$$\mathcal{D} = \int_\Omega \frac{\partial\varphi}{\partial\dot{\mathbf{p}}}(\boldsymbol{x}, \dot{\mathbf{p}}) \cdot \dot{\mathbf{p}}\, \mathrm{d}V, \tag{6}$$

where $\varphi$ is a convex, positive function of the irreversible polarization rate $\dot{\mathbf{p}}$ such that $\varphi(\cdot, \mathbf{0}) = 0$, which can be used to characterize dissipative processes such as microscopic domain switching in ferroelectrics. The form (6) guarantees positive dissipation.

Thermodynamic arguments then imply that the constitutive relations of the material are given by (see Bassiouny *et al* 1988)

$$\boldsymbol{E} = \frac{\partial E}{\partial \boldsymbol{P}}(\boldsymbol{x}, \boldsymbol{P}, \mathbf{p}) \qquad \text{and} \qquad \frac{\partial E}{\partial \mathbf{p}}(\boldsymbol{x}, \boldsymbol{P}, \mathbf{p}) + \frac{\partial\varphi}{\partial\dot{\mathbf{p}}}(\boldsymbol{x}, \dot{\mathbf{p}}) = \mathbf{0}, \tag{7}$$

[2] For typical ferroelectric composites, the overall dielectric response under stress-free conditions is not expected to be greatly affected by the local electromechanical coupling.

where the first expression gives the relation between the electric field and the polarization and the last expression provides the evolution law for the irreversible polarization $\mathbf{p}$. These constitutive relations conform to the so-called generalized standard material model of Rice (1971) and Halphen and Nguyen (1975). In the case of nonsmooth potentials, the derivatives in (7) should be understood in the sense of the subdifferential of convex analysis.

Now, electrostatic problems are more conveniently formulated in terms of a free energy density defined as

$$\psi(\boldsymbol{x}, \boldsymbol{E}, \mathbf{p}) \doteq \sup_{\boldsymbol{P}} [\boldsymbol{E} \cdot \boldsymbol{P} - E(\boldsymbol{x}, \boldsymbol{P}, \mathbf{p})] + \tfrac{1}{2}\epsilon_0 \boldsymbol{E}^2, \tag{8}$$

where the first term corresponds to a partial Legendre transformation of $E$ with respect to $\boldsymbol{P}$. Note that the function $\psi$ is thus convex in $\boldsymbol{E}$ but concave in $\mathbf{p}$. The constitutive relations (7) can then be written as

$$\boldsymbol{D} = \frac{\partial \psi}{\partial \boldsymbol{E}}(\boldsymbol{x}, \boldsymbol{E}, \mathbf{p}) \qquad \text{and} \qquad \frac{\partial \psi}{\partial \mathbf{p}}(\boldsymbol{x}, \boldsymbol{E}, \mathbf{p}) - \frac{\partial \varphi}{\partial \dot{\mathbf{p}}}(\boldsymbol{x}, \dot{\mathbf{p}}) = \mathbf{0}, \tag{9}$$

where the polarization $\boldsymbol{P}$ has been eliminated in favor of the electric field $\boldsymbol{E}$. Making use of the characteristic functions $\chi^{(r)}$, the potentials $\psi$ and $\varphi$ are finally expressed as

$$\psi(\boldsymbol{x}, \boldsymbol{E}, \mathbf{p}) = \sum_{r=1}^{2} \chi^{(r)}(\boldsymbol{x})\, \psi^{(r)}(\boldsymbol{E}, \mathbf{p}), \qquad \varphi(\boldsymbol{x}, \dot{\mathbf{p}}) = \sum_{r=1}^{2} \chi^{(r)}(\boldsymbol{x})\, \varphi^{(r)}(\dot{\mathbf{p}}), \tag{10}$$

where $\psi^{(r)}$ and $\varphi^{(r)}$ denote, respectively, the free energy densities and dissipation potentials of each phase $r$.

The field equations and boundary conditions (1)–(4), together with the constitutive relations (9)–(10) and appropriate initial conditions, completely define the electrostatic response of the system under consideration.

### *2.2. Some material responses*

Even though the approach considered in this work allows for general stored energy densities $E^{(r)}$ and dissipation potentals $\varphi^{(r)}$, it proves useful to record at this point some specific forms of common use.

Many nonpolar solids can be characterized as ideal isotropic dielectrics with a non-dissipative linear response; in this case, the potentials are of the form

$$E^{(r)}(\boldsymbol{P}, \mathbf{p}) = \tfrac{1}{2}\kappa^{(r)} \boldsymbol{P}^2 \qquad \text{and} \qquad \varphi^{(r)}(\dot{\mathbf{p}}) = 0, \tag{11}$$

where $\kappa^{(r)}$ is a positive material parameter characterizing the polarizability of the material; the corresponding free energy density is given by

$$\psi^{(r)}(\boldsymbol{E}, \mathbf{p}) = \tfrac{1}{2}\epsilon^{(r)} \boldsymbol{E}^2, \tag{12}$$

where $\epsilon^{(r)} \doteq \epsilon_0 + \kappa^{(r)^{-1}}$ represents the permittivity of the material. A perfect conductor where the electric field must vanish is characterized by the limiting case $\kappa^{(r)} \to 0$ ($\epsilon^{(r)} \to \infty$).

On the other hand, polycrystalline polar solids exhibiting isotropic ferroelectricity are commonly characterized by potentials of the form—see, for instance, Kamlah (2001) and Miehe and Rosato (2011)—

$$E^{(r)}(\boldsymbol{P}, \mathbf{p}) = \frac{1}{2}\kappa^{(r)}(\boldsymbol{P} - \mathbf{p})^2 + E^{(r)}_{\mathrm{st}}(\mathbf{p}), \qquad \varphi^{(r)}(\dot{\mathbf{p}}) = e^{(r)}_{\mathrm{c}} |\dot{\mathbf{p}}| + \frac{e^{(r)}_0 \dot{p}^{(r)}_0}{1 + m^{(r)}} \left( \frac{|\dot{\mathbf{p}}|}{\dot{p}^{(r)}_0} \right)^{1+m^{(r)}} \tag{13}$$

with

$$E_{\rm st}^{(r)}(\mathbf{p}) = -h_0^{(r)} p_{\rm s}^{(r)^2} \left[ \ln\left(1 - \frac{|\mathbf{p}|}{p_{\rm s}^{(r)}}\right) + \frac{|\mathbf{p}|}{p_{\rm s}^{(r)}} \right], \tag{14}$$

where $E_{\rm st}^{(r)}$ and $\varphi^{(r)}$ represent the energy stored and dissipated via microdomain switching. In the dissipation potential $(13)_2$, $e_{\rm c}^{(r)}$ is the coercive field strength of the material—i.e. the electric field level above which domain switching is triggered—, $e_0^{(r)}$ and $\dot{p}_0^{(r)}$ are the reference electric field and polarization rate-characterizing the rate dependence of the switching process and $m^{(r)}$ is a rate-sensitivity exponent. In the stored energy density (14), in turn, $p_{\rm s}^{(r)}$ is the saturation polarization and $h_0^{(r)}$ is a material parameter characterizing the hysteresis slope. The corresponding free energy density is given by

$$\psi^{(r)}(\boldsymbol{E}, \mathbf{p}) = \tfrac{1}{2}\epsilon^{(r)}\boldsymbol{E}^2 + \boldsymbol{E}\cdot\mathbf{p} - E_{\rm st}^{(r)}(\mathbf{p}), \tag{15}$$

where, again, $\epsilon^{(r)} = \epsilon_0 + \kappa^{(r)^{-1}}$ represents the permittivity of the material. In the limit $e_{\rm c}^{(r)} \to \infty$, this model reduces to the ideal dielectric described previously.

## 3. The overall response

The focus of this work is on material systems where the characteristic size of the microstructural heterogeneities—e.g. particles—is much smaller than the characteristic size of the composite body and the scale of variation of the boundary conditions. In this case, we can define an overall response of the composite material as the relation between conjugate fields averaged over a 'representative volume element' (RVE) $\Xi$ which contains a sufficient number of heterogeneities for the overall response to be effectively independent of the prevalent conditions on its boundary $\partial\Xi$, so long as the conditions are macroscopically uniform. This notion of RVE was made precise by Hill (1963) in the context of linearly elastic composites, and its range of validity in the broader context of generalized standard materials has been discussed by Germain *et al* (1983).

The determination of the overall response thus requires the solution to the above field equations for some choice of macroscopically uniform boundary conditions on the surface of the RVE. Also following the work of Hill (1963) in this regard, we choose the affine boundary conditions

$$\phi = -\overline{\boldsymbol{E}}\cdot\boldsymbol{x} \qquad \text{on } \partial\Xi. \tag{16}$$

Application of Gauss' theorem then shows that the volume average of the field $\boldsymbol{E}$ over the domain $\Xi$ occupied by the RVE is precisely $\overline{\boldsymbol{E}}$. An additional consequence of the condition (16) is that the solution to the field equations within $\Xi$ becomes independent of the electric field external to $\Xi$.

We now make use of the variational representation for the overall response of Miehe (2002). In this representation the field equations (1)–(16) defined over the RVE are discretized in time ($t_0 = 0, t_1, \ldots, t_n, t_{n+1}, \ldots, t_N = T$) following an implicit Euler scheme, so that the fields $\phi_{n+1}$ and $\mathbf{p}_{n+1}$ at time $t_{n+1}$ are solution to

$$\boldsymbol{E}_{n+1} = -\nabla\phi_{n+1}, \qquad \nabla\cdot\boldsymbol{D}_{n+1} = 0 \qquad \text{in } \Xi, \tag{17}$$

$$\boldsymbol{D}_{n+1} = \frac{\partial\psi}{\partial\boldsymbol{E}}(\boldsymbol{x}, \boldsymbol{E}_{n+1}, \mathbf{p}_{n+1}), \quad \frac{\partial\psi}{\partial\mathbf{p}}(\boldsymbol{x}, \boldsymbol{E}_{n+1}, \mathbf{p}_{n+1}) - \frac{\partial\varphi}{\partial\dot{\mathbf{p}}}\left(\boldsymbol{x}, \frac{\mathbf{p}_{n+1} - \mathbf{p}_n}{\Delta t}\right) = \mathbf{0} \qquad \text{in } \Xi, \tag{18}$$

$$\phi_{n+1} = -\overline{\boldsymbol{E}}_{n+1}\cdot\boldsymbol{x} \qquad \text{on } \partial\Xi, \tag{19}$$

where $\phi_n$ and $\mathbf{p}_n$ are the known values of the fields at the previous instant $t_n$ and $\Delta t$ is the time step, which has been assumed to be fixed—i.e. independent of $n$—for simplicity. The key observation in the context of these equations is that the constitutive relations (18) can be written as

$$\boldsymbol{D}_{n+1} = \frac{\partial w}{\partial \boldsymbol{E}}(\boldsymbol{x}, \boldsymbol{E}_{n+1}; \mathbf{p}_n), \tag{20}$$

where $w$ is an incremental potential defined by

$$w(\boldsymbol{x}, \boldsymbol{E}; \mathbf{p}_n) \doteq \sup_{\mathbf{p}} \left[ \psi(\boldsymbol{x}, \boldsymbol{E}, \mathbf{p}) - \Delta t \, \varphi\left(\boldsymbol{x}, \frac{\mathbf{p} - \mathbf{p}_n}{\Delta t}\right)\right]. \tag{21}$$

This follows from the facts that $\psi$ is concave in $\mathbf{p}$ and $\varphi$ is convex in $\dot{\mathbf{p}}$, and that the Euler–Lagrange equations associated with the supremum in (21) at $\boldsymbol{E}_{n+1}$ are precisely the relations $(18)_2$ for $\mathbf{p}_{n+1}$. That the derivative of $w$ with respect to the electric field yields the electric displacement $\boldsymbol{D}_{n+1}$ follows immediately from $(18)_1$ and the stationarity of (21) with respect to $\mathbf{p}$. It is simple to show that the incremental potential $w$ is a convex function of $\boldsymbol{E}$.

Of course, the incremental potential admits the form

$$w(\boldsymbol{x}, \boldsymbol{E}; \mathbf{p}_n) = \sum_{r=1}^{2} \chi^{(r)}(\boldsymbol{x}) w^{(r)}(\boldsymbol{E}; \mathbf{p}_n), \tag{22}$$

where $w^{(r)}$ are incremental phase potentials defined similarly in terms of the potentials $\psi^{(r)}$ and $\varphi^{(r)}$. In particular, when the phase potential $\psi^{(r)}$ is of the form (15), the incremental phase potential is given by

$$w^{(r)}(\boldsymbol{E}; \mathbf{p}_n) = \frac{1}{2}\epsilon^{(r)}\boldsymbol{E}^2 + \sup_{\mathbf{p}} \left[ \boldsymbol{E}\cdot\mathbf{p} - E^{(r)}_{\mathrm{st}}(\mathbf{p}) - \Delta t \, \varphi^{(r)}\left(\frac{\mathbf{p} - \mathbf{p}_n}{\Delta t}\right)\right], \tag{23}$$

which is a strictly convex function of $\boldsymbol{E}$. Note that the second term in this expression is the Legendre transform of the function $(E^{(r)}_{\mathrm{st}} + \Delta t \, \varphi^{(r)})$ with respect to $\mathbf{p}$. When the function $E^{(r)}_{\mathrm{st}}$ is strictly convex, the optimal $\mathbf{p}$ is unique.

Given (20), the equations (17)–(19) adopt the form

$$\boldsymbol{E} = -\nabla\phi, \quad \nabla\cdot\boldsymbol{D} = \mathbf{0}, \quad \boldsymbol{D} = \frac{\partial w}{\partial \boldsymbol{E}}(\boldsymbol{x}, \boldsymbol{E}; \mathbf{p}_n) \qquad \text{in } \Xi, \tag{24}$$

$$\phi = -\overline{\boldsymbol{E}}\cdot\boldsymbol{x} \qquad \text{on } \partial\Xi, \tag{25}$$

where the subscript $n+1$ has been dropped to ease notation. For given $\mathbf{p}_n$ and prescribed $\overline{\boldsymbol{E}}$, these equations provide the electrostatic fields at time $t_{n+1}$. Strict convexity of $w$ implies the field $\boldsymbol{E}$ is unique and locally bounded, and when the local potentials are of the form (23), the field $\mathbf{p}$ is also unique and locally bounded. Now, the system (24)–(25) are the Euler-Lagrange equations of the variational problem (Miehe 2002)

$$\widetilde{w}(\overline{\boldsymbol{E}}; \mathbf{p}_n) = \min_{\boldsymbol{E}\in\mathcal{K}(\overline{\boldsymbol{E}})} \left\langle w(\boldsymbol{x}, \boldsymbol{E}; \mathbf{p}_n)\right\rangle, \tag{26}$$

where $\langle\cdot\rangle$ denotes volume average over $\Xi$, and $\mathcal{K}(\overline{\boldsymbol{E}})$ denotes the set of fields $\boldsymbol{E} : \Xi \to \mathbb{R}^3$ such that there exists a continuous field $\phi : \Xi \to \mathbb{R}$ satisfying $(24)_1$ in $\Xi$ and (25) on $\partial\Xi$. It then follows from Hill's lemma that

$$\overline{\boldsymbol{D}} = \frac{\partial \widetilde{w}}{\partial \overline{\boldsymbol{E}}}(\overline{\boldsymbol{E}}; \mathbf{p}_n), \tag{27}$$

where $\overline{\boldsymbol{D}} = \langle\boldsymbol{D}\rangle$ and $\overline{\boldsymbol{E}} = \langle\boldsymbol{E}\rangle$. Thus, this expression relates the averages of the electric displacement and electric fields over $\Xi$, and therefore constitutes the overall response of the composite material in the sense of Hill (1963). The overall potential $\widetilde{w}$ represents the

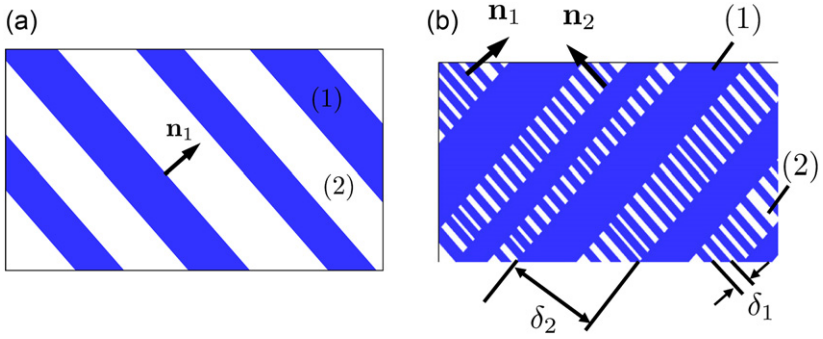


**Figure 1.** Two-phase laminates: (*a*) simple or rank 1 laminate, (*b*) rank 2 laminate ($\delta_2 \gg \delta_1$).

volume average of the local potential $w$, and completely characterizes the overall instantaneous response at time $t_{n+1}$. It can be shown that (strict) convexity of the local potential $w$ in $\boldsymbol{E}$ implies (strict) convexity of the overall potential $\widetilde{w}$ in $\overline{\boldsymbol{E}}$ (Ponte Castañeda and Willis 1988). Note that despite appearances, equations (22)–(24) do not correspond strictly to a two-phase composite but rather to a composite with an infinite number of phases. This is because the field $\mathbf{p}_n$ is, in general, heterogeneous even within each constituent phase. However, a key observation for the iterative scheme of the next section is that expression (26) is actually valid for any material response of the form $(24)_3$, which, in view of (27), includes the overall response.

Finally, the macroscopic fields associated with the problem (1)–(4) at time $t_{n+1}$ are given by

$$\nabla \cdot \overline{\boldsymbol{D}} = 0 \qquad \text{and} \qquad \overline{\boldsymbol{E}} = -\nabla\overline{\phi} \qquad \text{in } \mathbb{R}^3, \tag{28}$$

$$\overline{\phi} = \hat{\phi} \quad \text{on } \partial\Omega_v \qquad \text{and} \qquad [\overline{\boldsymbol{D}} \cdot \boldsymbol{n}] = 0 \qquad \text{on } \partial\Omega \backslash \partial\Omega_v, \tag{29}$$

with the constitutive relation (27).

## 4. A sequentially laminated model for particulate composites

We now derive an expression for the overall potential $\widetilde{w}$ of a special class of sequentially laminated microgeometries representing particulate composites. A sequential laminate is an iterative construction obtained by layering laminated materials (which in turn have been obtained from lower-order lamination procedures) with other laminated materials, or directly with the homogeneous phases that make up the composite (see, for example, Milton 2002). The *rank* of the laminate refers to the number of layering operations required to reach the final sequential laminate. It will turn out that the number of internal variables appearing in the overall potential is finite and dictated by its rank. Throughout this section a subscript $k$ is used to denote quantities corresponding to the rank-$k$ laminate.

Given our interest in two-phase composites comprising a continuous matrix containing a random dispersion of inclusions, we follow the work of Idiart (2006, 2008). Thus, a sequence is formed by layering a laminate with the matrix material at every step, here identified with $r = 1$. In this sequence, a rank-1 laminate corresponds to a simple laminate with a given layering direction $\boldsymbol{n}_1$, with phases 1 and 2 in proportions $(1 - f_1)$ and $f_1$, as shown in figure 1(*a*). The characteristic functions describing these microgeometries depend on $\boldsymbol{x}$ only through the combination $\boldsymbol{x} \cdot \boldsymbol{n}_1$. Now, the mathematical structure of the minimization problem (26) is analogous to that of non-dissipative two-phase dielectrics. It then follows that the exact electric field in a simple laminate, subjected to affine boundary conditions (16), is uniform per

phase. The overall potential $\widetilde{w}_1$ of the rank-1 laminate has been given by Ponte Castañeda (1992) and can be written as

$$\widetilde{w}_1(\overline{\boldsymbol{E}}; \mathbf{p}^{(1)}_{n,1}, \mathbf{p}^{(2)}_n) = \min_{a_1} \left\{ f_1 w^{(2)} \left( \overline{\boldsymbol{E}} - (1-f_1) a_1 \boldsymbol{n}_1; \mathbf{p}^{(2)}_n \right) + (1-f_1)\, w^{(1)} \left( \overline{\boldsymbol{E}} + f_1 a_1 \boldsymbol{n}_1; \mathbf{p}^{(1)}_{n,1} \right) \right\}. \tag{30}$$

In this expression, the arguments of the potentials $w^{(r)}$ represent the local electric fields in each phase $r$, and the minimization with respect to the scalar $a_1$ enforces continuity of electric displacement accross the internal material interfaces. Note that the irreversible polarization field will also be uniform per phase provided it is initially so. Under this assumption, the tensors $\mathbf{p}^{(1)}_{n,1}$ and $\mathbf{p}^{(2)}_n$ represent the values at time $t_n$ of the irreversible polarization in phases 1 and 2, respectively. Thus, the overall response depends on the macroscopic electric field and two internal variables.

A rank-2 laminate is constructed by layering the rank-1 laminate with phase 1, along a layering direction $\boldsymbol{n}_2$, in proportions $f_2$ and $1-f_2$, as shown schematically in figure 1(*b*). The key assumption in this construction process is that the length scale of the *embedded* laminate is taken to be much smaller than the length scale of the *embedding* laminate, *i.e.*, $\delta_1 \ll \delta_2$ in figure 1(*b*). According to the iterated homogenization theorem (e.g. Braides and Lukkassen 2000), the overall potential $\widetilde{w}_2$ of the rank-2 laminate is then given by the formula (30) for a simple laminate, with the potential $w^{(2)}$ replaced by $\widetilde{w}_1$, and the potential $w^{(1)}$ evaluated at a different irreversible polarization $\mathbf{p}^{(1)}_{n,2}$. Note that the total concentration of material $r=2$ in the two-scale rank-2 laminate is $f_1 f_2$. The resulting expression for the overall response depends on three internal variables.

A rank-$M$ laminate is obtained by repeating this process $M$ times, always laminating a rank-$m$ laminate with material $r=1$, in proportions $f_m$ and $(1-f_m)$, respectively, along a layering direction $\boldsymbol{n}_m$. Making repeated use of the formula (30) for simple laminates, it can be shown—see Idiart (2008) for a derivation in the context of viscoplasticity—that the overall potential $\widetilde{w}_M$ of the rank-$M$ laminate is given by

$$\widetilde{w}_M(\overline{\boldsymbol{E}}; \mathbf{p}^{(1)}_{n,i}, \mathbf{p}^{(2)}_n) = \min_{\substack{a_i \\ i=1,\dots,M}} \left\{ c^{(2)} w^{(2)} \left( \overline{\boldsymbol{E}}^{(2)}; \mathbf{p}^{(2)}_n \right) + c^{(1)} \sum_{i=1}^{M} \theta_i\, w^{(1)} \left( \overline{\boldsymbol{E}}^{(1)}_i; \mathbf{p}^{(1)}_{n,i} \right) \right\}, \tag{31}$$

where

$$c^{(2)} = 1 - c^{(1)} = \prod_{i=1}^{M} f_i \quad \text{and} \quad \theta_i = \frac{(1-f_i)}{f_i} \frac{\prod_{j=i}^{M} f_j}{1 - \prod_{j=1}^{M} f_j} \tag{32}$$

are microstructural variables representing, respectively, the total volume fractions of each material $r$—such that $c^{(1)} + c^{(2)} = 1$—and the fraction of matrix material added at the $i^{th}$ lamination—such that $\theta_i > 0$ and $\sum_{i=1}^{M} \theta_i = 1$—and the vectors $\overline{\boldsymbol{E}}^{(1)}_i$ and $\overline{\boldsymbol{E}}^{(2)}$ are local fields given by

$$\overline{\boldsymbol{E}}^{(1)}_i = \overline{\boldsymbol{E}} + a_i \boldsymbol{n}_i - \sum_{j=i}^{M} (1-f_j)\, a_j \boldsymbol{n}_j, \qquad i = 1, \dots, M, \tag{33}$$

$$\overline{\boldsymbol{E}}^{(2)} = \overline{\boldsymbol{E}} - \sum_{j=1}^{M} (1-f_j)\, a_j \boldsymbol{n}_j. \tag{34}$$

Thus, the overall response (31) involves $M+1$ internal variables; its computation requires the solution of a convex optimization problem with respect to $M$ scalars $a_i$. Note that the potential $w^{(2)}$ is evaluated at a single value of the electric field and irreversible polarization,

which means that the fields in phase $r = 2$ are uniform. The potential $w^{(1)}$, by contrast, is evaluated at $M$ different values of the fields, which means that fields are heterogeneous within phase $r = 1$. This field heterogeneity can be described in terms of its statistics. In particular, the volume average and standard deviation of the electric field in the matrix phase can be computed as

$$\overline{\boldsymbol{E}}^{(1)} = \sum_{i=1}^{M} \theta_i \overline{\boldsymbol{E}}_i^{(1)} \quad \text{and} \quad SD^{(1)}(E) = \left[ \sum_{i=1}^{M} \theta_i |\overline{\boldsymbol{E}}_i^{(1)}|^2 - |\overline{\boldsymbol{E}}^{(1)}|^2 \right]^{1/2}. \tag{35}$$

Statistics of the polarization fields can be computed similarly.

In the above sequentially laminated constructions the discontinuous inclusion phase is made up of material $r = 2$ while the continuous matrix phase is made up of material $r = 1$, see figure 1(*b*). Their overall potential $\widetilde{w}_M$ depends on the total volume fractions $c^{(r)} = \langle \chi^{(r)}(\boldsymbol{x}) \rangle$ of each phase $r$ and on higher-order microstructural correlations through the set of microstructural quantities $\{(f_i, \boldsymbol{n}_i), i = 1, \ldots, M\}$. Thus, in order to use these constructions as model composites, the quantities $(f_i, \boldsymbol{n}_i)$ must be expressed in terms of the multi-point correlations of the microgeometries. However, this is not feasible in general. One strategy consists then in identifying subclasses of sequentially laminated constructions for which the dependence of the overall potential on higher-order correlations can be made explicit (Idiart 2008, Idiart and Ponte Castañeda 2013). Another strategy consists in identifying subclasses for which the overall potential exhibits desirable characteristics such as a certain symmetry group (deBotton and Hariton 2002, Danas *et al* 2008a, 2008b). In any event, it proves convenient to relate the quantities $(f_i, \boldsymbol{n}_i)$ to the so-called $H$-measures of the microgeometry. These measures are geometrical objects that depend on the two-point correlation functions $\langle \chi^{(r)}(\boldsymbol{x}) \chi^{(s)}(\boldsymbol{x} - \boldsymbol{y}) \rangle$ of the microstructure; they quantify in phase space the lack of compactness of weakly converging sequences of characteristic functions $[\chi^{(r)}(\boldsymbol{x}) - c^{(r)}]$ and provide a partial characterization of microstructural oscillations along different directions in physical space (Tartar 1990, Gérard 1991). Explicit expressions for periodic and random microstructures can be found in Kohn (1991) and Smyshlyaev and Willis (1998), respectively.

The reduced $H$-measure of the above sequential laminates is given by—see, for instance, Idiart and Ponte Castañeda (2013)—

$$\overline{\nu}_M(\boldsymbol{n}) = \sum_{i=1}^{M} \nu_i \, \delta(\boldsymbol{n} - \boldsymbol{n}_i), \qquad \text{with} \quad \nu_i = \frac{1}{c^{(1)}} \frac{1 - f_i}{f_i} \prod_{j=1}^{i} f_j, \tag{36}$$

where $\delta(\cdot)$ denotes the vector-valued Dirac delta function, and the quantities $\nu_i$ are such that

$$\nu_i \geqslant 0 \qquad \text{and} \qquad \sum_{i=1}^{M} \nu_i = 1. \tag{37}$$

Relations $(36)_2$ can be inverted to express the $f_i$ in terms of the $\nu_i$ as

$$f_i = \frac{1 - c^{(1)} \left( 1 + \nu_i - \sum_{j=i}^{M} \nu_j \right)}{1 - c^{(1)} \left( 1 - \sum_{j=i}^{M} \nu_j \right)}. \tag{38}$$

Upon replacing the $f_i$ in (31)–(34) by (38), we obtain an alternative expression for the overall potential $\widetilde{w}_M$ that depends on the underlying microgeometry through the total volume fractions $c^{(r)}$ of each material $r$ and the set $\{(\nu_i, \boldsymbol{n}_i)\}$ subject to the constraints (37). Note that

**Table 1.** Parameters for the ferroelectric material. These values roughly reproduce the rate-dependent behavior of a polycrystalline lead zirconate titanate at low frequencies (e.g. Zhou *et al* (2001), Miehe and Rosato (2011)).

| Symbol | Parameter | Units | Value |
|---|---|---|---|
| $\epsilon$ | Electric permittivity | $\mathrm{C\,(V^{-1}m^{-1})}$ | $1800\epsilon_0$ |
| $p_s$ | Saturation polarization | $\mathrm{C\,m^{-2}}$ | 0.25 |
| $h_0$ | Hysteresis slope | $\mathrm{MV\,m\,C^{-1}}$ | 0.1 |
| $m$ | Rate-sensitivity exponent | — | 0.2 |
| $\dot{p}_0$ | Reference polarization rate | $\mathrm{C\,(m^{-1}s^{-1})}$ | 100 |
| $e_c$ | Coercive electric field | $\mathrm{MV\,m^{-1}}$ | 0.35 |
| $e_0$ | Reference electric field | $\mathrm{MV\,m^{-1}}$ | 0.35 |

the reduced $H$-measure $\overline{\nu}_M(\boldsymbol{n})$ is fully determined by the set, but the set is not fully determined by the reduced $H$-measure $\overline{\nu}_M$. This is due to the fact that there is no one-to-one correspondence between the function $\overline{\nu}_M(\boldsymbol{n})$ and the $\nu_i$ when lamination sequences involve repeated lamination directions, and that the function $\overline{\nu}_M$ is insensitive to the order of the elements in the set. The overall potential $\widetilde{w}_M$ therefore depends, in general, on microstructural information *beyond* the volume fractions and the $H$-measure. In any event, the quantities $\nu_i$ do provide a convenient means of identifying appropriate lamination sequences, as will be seen in the next section.

That these material systems represent the essential features of two-phase composites with particulate microstructures is supported by comparisons with full-field simulations and approximate estimates reported in various works on purely energetic/dissipative composites (e.g. deBotton and Hariton (2002), Idiart (2006, 2008), Danas *et al* (2008a, 2008b)). Furthermore, when both phases are ideal dielectrics, the potential (31) agrees exactly with the Maxwell-Garnett approximation—also known as the Claussius-Mossotti approximation—for two-phase linear dielectrics with $H$-measure $(36)_1$. The resulting predictions are therefore expected to be particularly relevant to composites with polydispersed particle distributions.

## 5. Sample results for representative material systems

The model presented above is used in this section to explore the effects of material heterogeneity on the electrostatic response of ferroelectric composites with particulate microstructures. Three material systems of particular relevance are considered: (i) an ideal dielectric containing a random dispersion of ferroelectric particles, (ii) a ferroelectric material containing a random dispersion of perfectly conducting particles and (iii) a ferroelectric material with porosity. In all cases, the ferroelectric material is characterized by potentials of the form (13)–(15). Table 1 shows the numerical values employed in the simulations for the various material parameters; these values roughly reproduce the rate-dependent behavior of a polycrystalline lead zirconate titanate at low frequencies (e.g. Zhou *et al* (2001), Miehe and Rosato (2011)). The ideal dielectric and the perfect conductor are in turn characterized by potentials of the form (11)–(12) with finite ($0 < \epsilon^{(r)} < +\infty$) and infinite ($\epsilon^{(r)} \to \infty$) permittivities, respectively, while voids are assumed to be vacuous ($\epsilon^{(r)} = \epsilon_0$). It is recalled that for these material systems the local fields $\boldsymbol{E}$ and $\mathbf{p}$ are unique and bounded.

We focus on material systems exhibiting overall isotropic symmetry. Motivated by the works of deBotton and Hariton (2002) and Idiart (2006) (see also Danas *et al* (2008b)), we

adopt the following lamination sequence:

$$v_i = \frac{1}{M}, \tag{39}$$

$$\boldsymbol{n}_i = \sin\alpha_i \sin\beta_i\ \boldsymbol{e}_1 + \cos\alpha_i \sin\beta_i\ \boldsymbol{e}_2 + \cos\beta_i\ \boldsymbol{e}_3, \quad i = 1, \ldots, M, \tag{40}$$

where

$$\beta_{j+kM_\eta} = \arccos h_j, \quad h_j = 2\frac{j-1}{M_\eta - 1} - 1, \quad j = 1, ..., M_\eta, \quad k = 0, ..., \eta - 1, \tag{41}$$

and (42)

$$\alpha_1 = \alpha_{M_\eta} = 0, \tag{43}$$

$$\alpha_{j+kM_\eta} = \left(\alpha_{j-1} + \frac{3.6}{\sqrt{M_\eta}}\frac{1}{\sqrt{1-h_j^2}}\right) \bmod 2\pi, \quad j = 2, \ldots, M_\eta - 1, \quad k = 0, \ldots, \eta - 1. \tag{44}$$

In these expressions, the angles $\alpha_i$ and $\beta_i$ determine the $i$th direction of lamination relative to a reference basis $\{\boldsymbol{e}_i\}$, and the parameters $\eta$ and $M_\eta$ are two integers such that the rank of the laminate is $M = \eta M_\eta$. The set of angles (41)–(44) corresponds to $M_\eta$ lamination directions $(40)_1$ uniformly distributed on the unit sphere (Saff and Kuijlaars 1997), with $\eta$ laminations for each direction. In turn, the quantities $v_i$ are set all equal and satisfy the constraints (37). This is a sequence for which the $H$-measure becomes isotropic as $M_\eta \to \infty$, for any number of rounds $\eta$. However, the resulting microgeometries in that limit are not isotropic. In order to generate material systems exhibiting overall isotropic responses, the second limit $\eta \to \infty$ must also be taken—the reader is referred to Idiart and Ponte Castañeda (2013) for a more detailed discussion on this point. It has been verified numerically that, for the materials considered here, the overall response becomes progressively less sensitive to the orientation of applied electric field $\overline{\boldsymbol{E}}$ as the parameters $M_\eta$ and $\eta$ increase; the values $\eta = 5$ and $M_\eta = 50$, which correspond to sequential laminates of rank $M = 250$, have been found adequate for the purposes of this work[3].

The results reported below correspond to initially unpoled (i.e. $\mathbf{p} = \mathbf{0}$) material systems subjected to a triangular electric signal along the $\mathbf{e}_1$ direction at a frequency $f_0$ of 1 Hz. For each value of applied electric field $\overline{\boldsymbol{E}}$, the minimization in (31) with respect to the $M$ scalars $a_i$ is solved by means of a quasi-Newton optimization method for smooth, convex functions, while the irreversible polarizations in the potentials $w^{(r)}$ are computed by means of a direct search complex algorithm for nonsmooth, convex functions. In the case of conducting inclusions, the minimization with respect to the $a_i$ is subject to the vectorial linear constraint $\overline{\boldsymbol{E}}^{(2)} = \mathbf{0}$ with $\overline{\boldsymbol{E}}^{(2)}$ given by (34). The time step adopted in all calculations is $\Delta t = 10^{-3} f_0^{-1}$.

### *5.1. Ideal dielectric containing ferroelectric inclusions*

Figure 2 shows predictions for an ideal dielectric containing a random dispersion of ferroelectric inclusions at a volume fraction of $c^{(2)} = 0.25$. Two sets of curves are presented: the first set corresponds to a low-contrast composite where the matrix phase has the same permittivity as the inclusions, $\epsilon^{(1)} = \epsilon^{(2)}$, while the second set corresponds to a moderate-contrast composite where $\epsilon^{(1)} = 0.1\epsilon^{(2)}$. The peak amplitude of the applied electric signal is $40e_c$—$e_c$ being the coercive electric field of the ferroelectric phase.

[3] Thus, the model involves 251 internal (vector) variables.

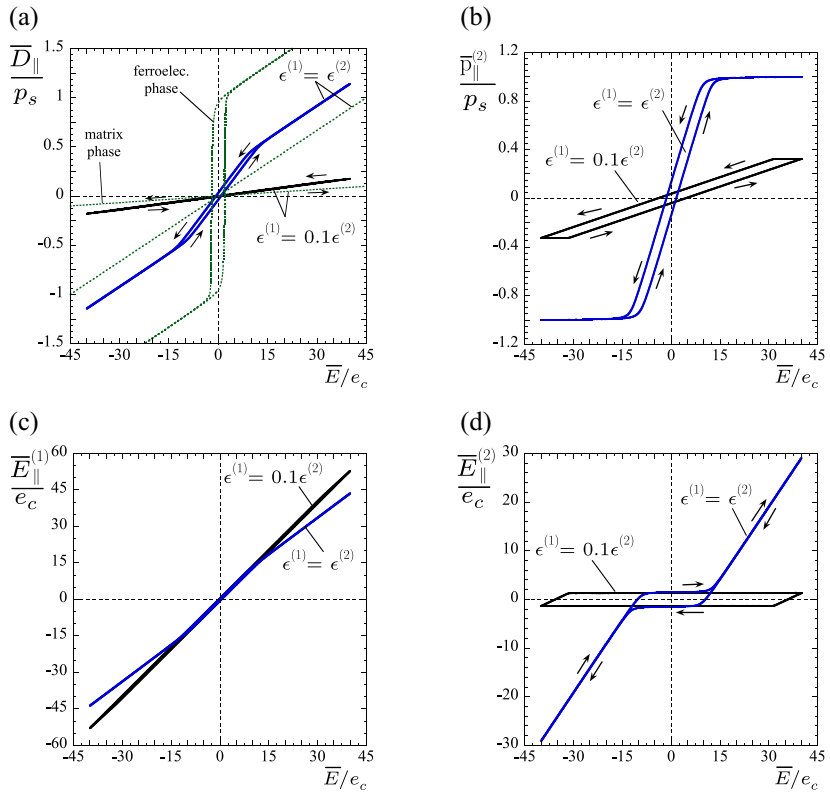


**Figure 2.** Predictions for an ideal dielectric matrix containing a random dispersion of ferroelectric inclusions at a volume fraction of $c^{(2)} = 0.25$. The composite is subjected to a triangular electric signal with a peak amplitude of $40e_c$ and a frequency of 1 Hz. Normalized vector components along the direction of applied electric field ($\parallel$): (*a*) overall dielectric displacement, (*b*) average irreversible polarization in the inclusions, (*c*) and (*d*) average electric field in the matrix ($r = 1$) and inclusion ($r = 2$) phases.

Plots versus the applied electric field ($\overline{E}$) are given for the (*a*) overall electric displacement ($\overline{D}_{\parallel}$), the (*b*) average irreversible polarization in the ferroelectric inclusions ($\overline{p}^{(2)}_{\parallel}$) and the (*c* and *d*) average electric field in the matrix ($\overline{E}^{(1)}_{\parallel}$) and inclusion ($\overline{E}^{(2)}_{\parallel}$) phases. Recall that the predicted fields in the inclusion phase are uniform. The dielectric responses of the monolithic phases are also included as a reference. The predictions for the low-contrast composite show a bilinear-type of overall cyclic response with low hysteresis. The change in slope occurs when the irreversible polarization in the inclusions reaches saturation, as expected. The predictions for the moderate-contrast composite, on the other hand, show a linear-type overall response because the polarization in the inclusions does not reach saturation within the range of applied fields considered. More important, however, is the fact that the polarization at a given intensity $\overline{E}$ decreases with decreasing permittivity ratio $\epsilon^{(1)}/\epsilon^{(2)}$. This is a consequence of the basic fact that the electric field—which provides the driving force for the evolution of polarization—always tends to concentrate in the phase with lowest permittivity—in this case, the matrix. The results for $\epsilon^{(1)} = 0.1\epsilon^{(2)}$ show that the polarization is far from saturation even for field intensities $\overline{E}$ as large as forty times the coercive strength $e_c$ of the ferroelectric phase. Note that at such intensities, the phase averages of the electric fields are already in the order of the

dielectric strengths expected for the constituent materials typically employed in this kind of composites[4]. Given that the electromechanical coupling of a ferroelectric material is roughly proportional to the amount of spontaneous polarization, this implies that composites with low permittivity ratios will always exhibit a very low coupling.

In practice, these kind of composites are made up of a polymeric matrix and ceramic inclusions. In that case, the permittivity ratio $\epsilon^{(1)}/\epsilon^{(2)}$ is well below 0.1, and so according to the present theoretical model the applied field intensities required for poling the ferroelectric particles would be exceedingly large. This seems to be at odds with the experimental measurements of Lam *et al* (2005). These authors have produced composite films comprised of a polyurethane matrix containing a random dispersion of lead zirconate titanate (PZT) particles at volume fractions in the range 0.05–0.3. The permittivity ratio in these composites is $\epsilon^{(1)}/\epsilon^{(2)} \approx 0.004$. Their through-thickness measurements of the overall strain versus applied electric field show meaningful deformations—which presumably requires significant spontaneous polarization densities in the ferroelectric inclusions—for field intensities as low as a few $\mathrm{MV\,m^{-1}}$. One possible source of discrepancy between these experimental observations and the theoretical model presented here could be attributed to the presence of interphase regions or interface charges surrounding the inclusions and causing an elevated electric field inside the inclusions. Interface phenomena typically result in a size-dependent overall response. Mao *et al* (2010) have recently reported measurements on a family of polyvinylidene fluoride (PVDF) composites containing monodispersed distributions of $BaTiO_3$ particles[5] at a volume fraction of 0.6 and characteristic sizes in the range 25–500 nm. These measurements do show a well-defined size effect, but the observed effect is contrary to the above speculation: larger particles result in larger polarizations at a given field intensity. Thus, further work is required to clarify this point. In any event, these observations shed caution on the use of the approach presented here—and other approaches expected to produce similar predictions—as it stands to model polymer-matrix ferroelectric composites.

### *5.2. Ferroelectric matrix containing perfectly conducting inclusions*

Figure 3 shows predictions for a ferroelectric matrix containing a random dispersion of perfectly conducting inclusions at a volume fraction of $c^{(2)} = 0.25$. The peak amplitude of the applied electric signal is $4e_c$.

Plots versus the applied electric field ($\overline{E}$) are given for the (*a*) overall electric displacement ($\overline{D}_\parallel$), the (*b*) average irreversible polarization in the ferroelectric matrix ($\overline{p}_\parallel^{(1)}$), and the (*c* and *d*) standard deviations ($\mathrm{SD}^{(1)}$) of the electric field and the irreversible polarization in the matrix phase. Recall that in these material systems $\overline{\boldsymbol{E}}^{(2)} = \boldsymbol{0}$, and therefore, by macroscopic balance, $\overline{\boldsymbol{E}}^{(1)} = \overline{\boldsymbol{E}}/c^{(1)}$. The dielectric response of the monolithic ferroelectric matrix is also included for reference. The predictions for the overall cyclic response show that the addition of conducting inclusions reduces the macroscopic coercive strength—i.e. the value of $\overline{E}$ for which $\overline{D}_\parallel = 0$— as expected from the fact that $|\overline{E}_\parallel^{(1)}| > |\overline{E}|$, but produces minimal changes in the macroscopic residual polarization—i.e. the value of $\overline{D}_\parallel$ at $\overline{E} = 0$. This is consistent with the experimental measurements of Duan *et al* (2000) on PZT composites containing a dispersion of Pt particles.

[4] Typical polymers used as the matrix, such as polyurethane and polysterene, exhibit dielectric strengths in the range $40e_c$–$60e_c$; corresponding values for typical ferroelectric ceramics, such as PZT and $BaTiO_3$, are in the order of $10e_c$–$30e_c$.

[5] In these composites, both the matrix and the particles exhibit ferroelectricity.

The predictions also show that, unlike the monolithic ferroelectric matrix, the composite exhibits a two-stage saturation beginning at roughly half the dielectric displacement of the total saturation. At that point, the fluctuations of the spontaneous polarization field, as measured by the standard deviation, reaches a maximum[6]. This maximum is a consequence of the pointwise bounds—as dictated by the saturation polarization $p_s$—the field $\mathbf{p}$ must satisfy. Additional results—not provided here for brevity—show that the two-stage saturation fades out with decreasing volume fraction of particles and increasing loading rate. Incidentally, a similar behavior can be observed in full-field simulations and experimental measurements on ferroelectric polycrystalline ceramics under suitable stress levels (Burcsu *et al* 2004, Zhang and Bhattacharya 2005a, 2005b). These are ferroelastic materials where mechanical stress—rather than particles—promotes a heterogeneous nucleation of spontaneous polarization. However, the precise underlying mechanism leading to the two-stage saturation has not yet been identified.

Finally, the predictions show that the standard deviation of the electric field in the matrix can be significant even at moderate values of the external field intensity. Of particular importance is the effect of these fluctuations on the field-induced evolution of the initial switching surface of the composite. This is a surface in $\overline{\boldsymbol{E}}$-space that delimits the set of external field vectors $\overline{\boldsymbol{E}}$ that do not change the spontaneous polarization within the composite. For the unpoled composite, the behavior is isotropic and therefore the surface is circular. Now, after the first hemicycle of the triangular loading considered in figure 3, the standard deviation of the residual electric field is seen to be approximately equal to the coercive strength $e_c$ of the ferroelectric matrix. Consequently, reloading the composite from this poled state along different directions is likely to produce changes in the spontaneous polarization at some point in the matrix at very small external field intensities, which implies, in turn, a very strong change in the initial switching surface of the composite. Note that such small external field intensities are accompanied by small average electric fields in the matrix in view of the relation $\overline{\boldsymbol{E}}^{(1)} = \overline{\boldsymbol{E}}/c^{(1)}$; the evolution of the initial switching surface is thus mostly governed by the intraphase field fluctuations. This shows that approximate methods based on linearizations of the local constitutive laws evaluated at the phase averages of the fields, such as the method of Huber *et al* (1999), can greatly overestimate initial switching surfaces in this kind of material systems.

### *5.3. Ferroelectric material with porosity*

Figure 4 shows predictions for a ferroelectric matrix containing a random dispersion of pores at a volume fraction of $c^{(2)} = 0.25$. The peak amplitude of the applied electric signal is $4e_c$.

Plots versus the applied electric field ($\overline{E}$) are given for the overall response and statistics of the fields. The predictions for the overall cyclic response show that the addition of porosity reduces the macroscopic residual polarization but produces minimal changes in the macroscopic coercive strength. This is indeed observed in the experimental measurements of Zeng *et al* (2007) and Nie *et al* (2010) on porous PZT ceramics. Thus, porosity produces the 'opposite' effect on the overall response to that produced by conducting particles. Note that the overall response in this porous material does not exhibit the two-stage saturation previously observed in composites with conducting particles. However, this feature does appear at larger levels of porosity—the results are not shown for brevity.

In turn, the predictions for the field statistics show that the average electric fields in each phase are roughly linear in the external field intensity, and that the fluctuations of the

[6] It is noted in passing that, unlike first-order averages, second-order averages take several loading cycles to reach the steady regime.

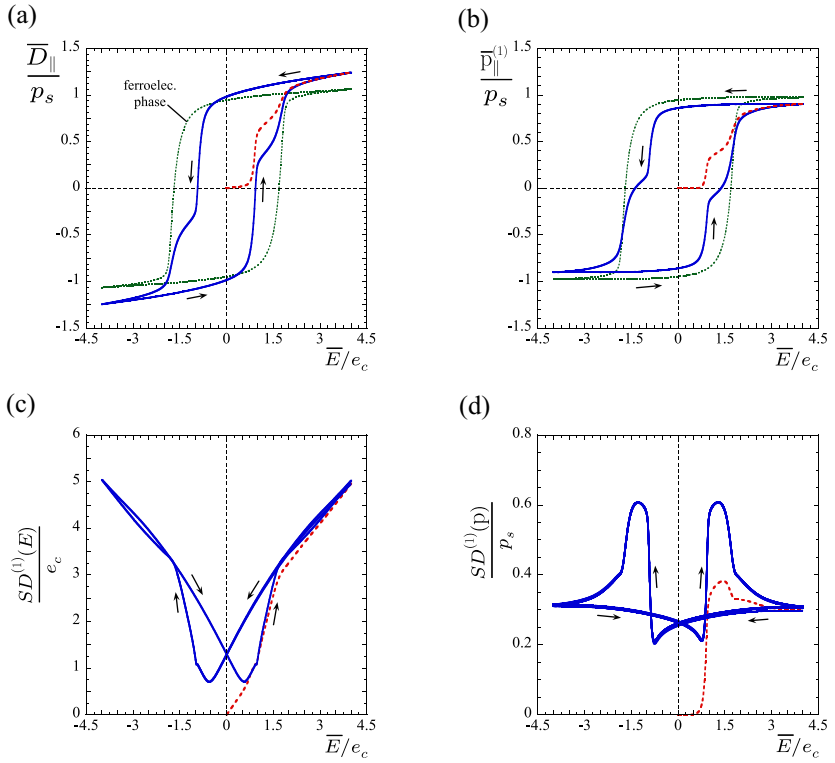


**Figure 3.** Predictions for a ferroelectric matrix containing perfectly conducting inclusions at a volume fraction $c^{(2)} = 0.25$. The composite is subjected to a triangular electric signal with a peak amplitude of $4e_c$ and a frequency of 1 Hz. Normalized vector components along the direction of applied electric field (‖): (*a*) overall dielectric displacement, (*b*) average irreversible polarization in the matrix. Normalized standard deviations in the matrix phase of the magnitudes of: (*c*) the electric field, (*d*) the irreversible polarization.

spontaneous polarization in the matrix phase during cyclic loading exhibit much smaller variations than in the case of composites with conducting particles. In addition, the intraphase fluctuations of the electric field do not decrease the external electric field intensity required for poling the composite. This situation persists at larger values of porosity. On the other hand, electric field fluctuations have been found to play a more important role in porous ferroelectrics with electrical creep responses of the type nucleation-growth-saturation, such as PLZT (Liu and Huber 2012). In that case, fluctuations may facilitate the poling process by reducing the required intensities of the external electric field. Given its capability of accounting for quite general material nonlinearities and local field fluctuations, the sequentially laminated model derived in this work should provide a convenient theoretical tool for studying such material systems.

## 6. Concluding remarks

In summary, sequentially laminated microgeometries prove a versatile tool for predicting the overall dissipative response of two-phase ferroelectric composites with complex particulate

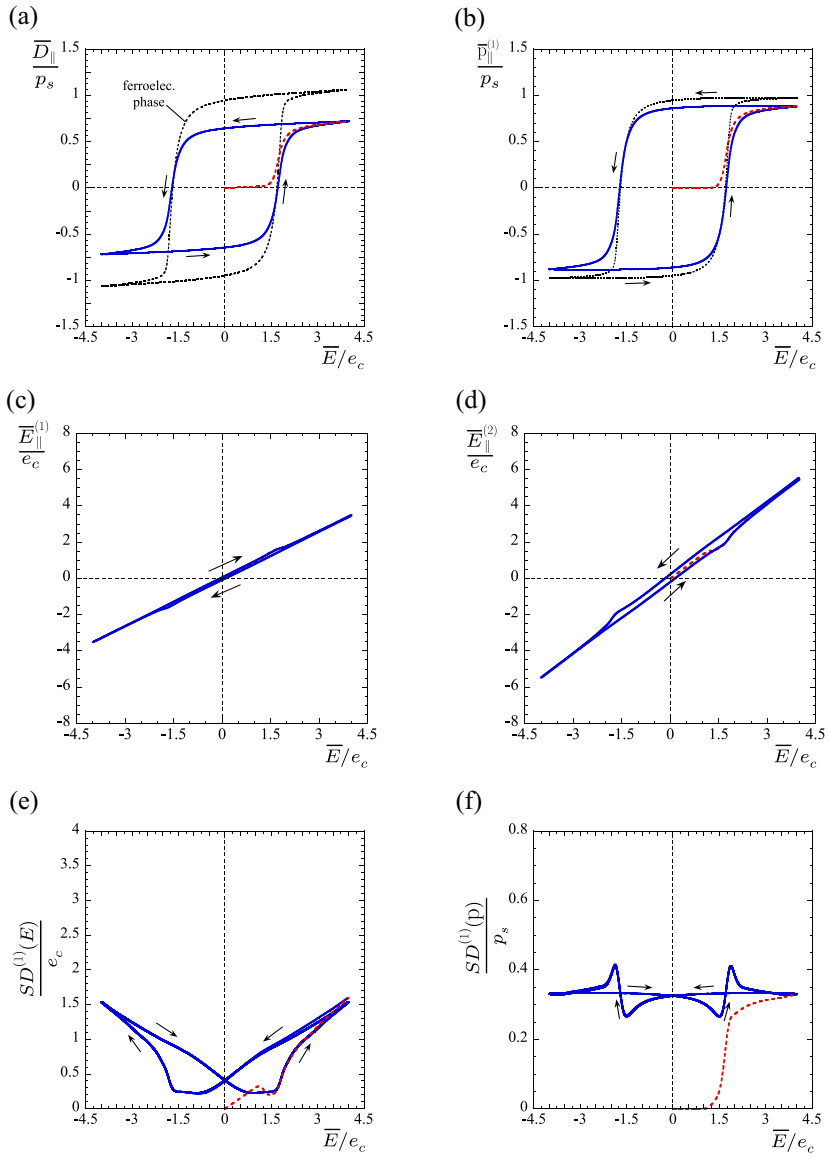


**Figure 4.** Predictions for a ferroelectric matrix containing a random dispersion of pores at a volume fraction $c^{(2)} = 0.25$. The porous material is subjected to a triangular electric signal with a peak amplitude of $4e_c$ and a frequency of 1 Hz. Normalized vector components along the direction of applied electric field ($\parallel$): (*a*) overall dielectric displacement, (*b*) average irreversible polarization in the matrix, (*c*) and (*d*) average electric field in the matrix ($\overline{E}^{(1)}_{\parallel}$) and inclusion ($\overline{E}^{(2)}_{\parallel}$) phases. Normalized standard deviations in the matrix phase of the magnitudes of: (*e*) the electric field, (*f*) the irreversible polarization.

microstructures under arbitrary loading histories. Statistics of the underlying field distributions within each phase can be predicted as well. Being realizable, the resulting estimates for the overall incremental potential always conform with material constraints, satisfy all pertinent bounds and exhibit the required convexity. Thus, they also provide convenient benchmarks

to test approximate methods such as those proposed by Lahellec and Suquet (2007a, 2007b, 2013) and Brassart *et al* (2011).

Even though the application was restricted here to material systems exhibiting overall isotropic symmetry, anisotropic systems can be modeled equally well by suitably choosing the lamination parameters $\{(\nu_i, \boldsymbol{n}_i)\}$. Of course, the predictive capability of the estimates proposed in this work is subordinate to the accuracy to which the phase potentials describe the dielectric response of the constituent phases. In the case of polycrystalline ferroelectric ceramics under complex loading histories, complicated behaviors resulting from the interplay between crystallographic texture and domain switching (e.g. Li *et al* 2005) may exceed the capabilities of the phenomenological models considered in this work, and may require 'micromechanical' constitutive models like those proposed by Huber *et al* (1999). Any such model can be used in the current approach provided they may be put in the incremental form $(24)_3$.

The encouraging results obtained in this work for the overall electrical response of ferroelectric composites motivate the application of similar ideas to estimate their overall electromechanical response. This possibility is currently being pursued.

## Acknowledgments

Part of this paper was written while the author was a guest in the Division of Engineering and Applied Science, California Institute of Technology (USA). Thanks are due to Professor K Bhattacharya for generous provision of facilities. Financial support from ANPCyT (Argentina) through grant PICT-2011-0167 is gratefully acknowledged.

## References

Asare T A, Poquette B D, Shultz J P and Kampe S L 2012 Investigating the vibration damping behavior of barium titanate ($BaTiO_3$) ceramics for use as a high damping reinforcement in metal matrix composites *J. Mater. Sci.* **47** 2573–82

Bassiouny E, Ghaleb A F and Maugin G A 1988 Thermodynamical formulation for coupled electromechanical hysteresis effects: I. Basic equations *Int. J. Eng. Sci.* **26** 1279–95

Braides A and Lukkassen D 2000 Reiterated homogenization of integral functions *Math. Models Methods Appl. Sci.* **10** 47–71

Brassart L, Stainier L, Doghri I and Delannay L 2011 A variational formulation for the incremental homogenization of elasto-plastic composites *J. Mech. Phys. Solids* **59** 2455–75

Bruggeman D A G 1935 Berechnung verschiedener physikalischer Konstanten von heterogenen Substanzen: I. Dielektrizitätskonstanten und Leitfähigkeiten der Mischkörper aus isotropen Substanzen *Ann. Phys.* **416** 636–64

Burcsu E, Ravichandran G and Bhattacharya K 2004 Large electrostrictive actuation of barium titanate single crystals *J. Mech. Phys. Solids* **52** 823–46

Capsal J-F, Charlotte D, Dantras E and Lacabanne C 2012 Piezoelectric sensing coating for real time impact detection and location on aircraft structures *Smart Mater. Struct.* **21** 055021

Chaboche J L, Kanouté P and Ross A 2005 On the capabilities of mean-field approaches for the description of plasticity in metal matrix composites *Int. J. Plast.* **21** 1409–34

Damjanovic D 2006 Hysteresis in piezoelectric and ferroelectric materials *The Science of Hysteresis* vol 3 ed I Mayergoyz and G Bertotti (Amsterdam: Elsevier)

Danas K, Idiart M I and Ponte Castañeda P 2008a A homogenization-based constitutive model for two-dimensional viscoplastic porous media *C. R. Mecanique* **336** 79–90

Danas K, Idiart M I and Ponte Castañeda P 2008b A homogenization-based constitutive model for isotropic viscoplastic porous media *Int. J. Solids Struct.* **45** 3392–409

deBotton G and Hariton I 2002 High-rank nonlinear sequentially laminated composites and their possible tendency towards isotropic behavior *J. Mech. Phys. Solids* **50** 2577–95

Duan N, ten Elshof J E and Verweij H 2000 Enhancement of dielectric and ferroelectric properties by addition of Pt particles to a lead zirconate titanate matrix *Appl. Phys. Lett.* **77** 3263–565

van den Ende D A, van de Wiel H J, Groen W A and van der Zwaag S 2012 Direct strain energy harvesting in automobile tires using piezoelectric PZT–polymer composites *Smart Mater. Struct.* **21** 015011

Gérard P 1991 Microlocal defect measures *Commun. Partial Diff. Eqns* **16** 1761–94

Germain P, Nguyen Q and Suquet P 1983 Continuum thermodynamics *J. Appl. Mech.* **50** 1010–20

Halphen B and Nguyen Q 1975 Sur les matériaux standard généralisés *J. Méc.* **14** 39–63

Hariton I and deBotton G 2003 The nearly isotropic behaviour of high-rank nonlinear sequentially laminated composites *Proc. R. Soc. Lond.* A **459** 157–74

Hill R 1963 Elastic properties of reinforced solids: some theoretical principles *J. Mech. Phys. Solids* **11** 357–72

Hill R 1965 Continuum micro-mechanics of elastoplastic polycrystals *J. Mech. Phys. Solids* **13** 89–101

Huber J E, Fleck N A, Landis C M and McMeeking R M 1999 A constitutive model for ferroelectric polycrystals *J. Mech. Phys. Solids* **47** 1663–97

Idiart M I 2006 Macroscopic behavior and field statistics in viscoplastic composites *PhD Thesis* University of Pennsylvania

Idiart M I 2008 Modeling the macroscopic behavior of two-phase nonlinear composites by infinite-rank laminates *J. Mech. Phys. Solids* **56** 2599–617

Idiart M I and Ponte Castañeda P 2013 Estimates for two-phase nonlinear conductors via iterated homogenization *Proc. R. Soc.* A **469** 20120626

Kamlah M 2001 Ferroelectric and ferroelastic piezoceramics—modelling of electromechanical hysteresis phenomena *Continuum Mech. Thermodyn.* **13** 219–68

Kohn R 1991 The relaxation of a double-well energy *Continuum Mech. Thermodyn.* **3** 193–236

Kovetz A 2000 *Electromagnetic Theory* (New York: Oxford)

Lahellec N and Suquet P 2004 Effective behavior of linear viscoelastic composites: a time-integration approach *Int. J. Solids Struct.* **44** 507–29

Lahellec N and Suquet P 2007a On the effective behavior of nonlinear inelastic composites: I. Incremental variational principles *J. Mech. Phys. Solids* **55** 1932–63

Lahellec N and Suquet P 2007b On the effective behavior of nonlinear inelastic composites: II. A second-order procedure *J. Mech. Phys. Solids* **55** 1964–92

Lahellec N and Suquet P 2013 Effective response and field statistics in elasto-plastic and elasto-viscoplastic composites under radial and non-radial loadings *Int. J. Plasticity* **42** 1–30

Lam K S, Zhou Y, Wong Y W and Shin F G 2005 Electrostriction of lead zirconate titanate/polyurethane composites *J. Appl. Phys.* **97** 104112

Li J Y, Rogan R C, Üstundag E and Bhattacharya K 2005 Domain switching in polycrystalline ferroelectric ceramics *Nature Mater.* **4** 776–81

Lines M E and Glass A M 1977 *Principles and Applications of Ferroelectrics and Related Materials* (Oxford: Oxford University Press)

Liu Q D and Huber J E 2012 Electrical creep around a circular hole in PLZT 8/65/35 *J. Eur. Ceram. Soc.* **32** 195–202

Mao Y P, Mao S Y, Ye Z-G, Xie Z X and Zheng L S 2010 Size-dependences of the dielectric and ferroelectric properties of $BaTiO_3$/polyvinylidene fluoride nanocomposites *J. Appl. Phys.* **108** 014102

Maxwell J C 1873 *A Treatise on Electricity and Magnetism* (Oxford: Claderon)

Miehe C 2002 Strain-driven homogenization of inelastic microstructures and composites based on an incremental variational formulation *Int. J. Numer. Method Eng.* **55** 1285–322

Miehe C and Rosato D 2011 A rate-dependent incremental variational formulation of ferroelectricity *Int. J. Eng. Sci.* **49** 466–96

Milton G W 2002 *The Theory of Composites* (Cambridge: Cambridge University Press)

Nie H C, Dong X L, Feng N B, Chen X F, Wang G S, Gu Y, He H L and Liu Y S 2010 Quantitative dependence of the properties of $Pb_{0.99}(Zr_{0.95}Ti_{0.05})_{0.98}Nb_{0.02}O_3$ ferroelectric ceramics on porosity *Mater. Res. Bull.* **45** 564–7

Ning X, Ping P Y and Zhuo W 2012 Large dielectric constant and Maxwell–Wagner effects in $BaTiO_3$/Cu composites *J. Am. Ceram. Soc.* **95** 999–1003

Olmos D, Martínez-Tarifa J M, González-Gaitano G and González-Benito J 2012 Uniformly dispersed submicrometre $BaTiO_3$ particles in PS based composites. Morphology, structure and dielectric properties *Polym. Test* **31** 1121–30

Ortiz M and Stainier L 1999 The variational formulation of viscoplastic constitutive updates *Comput. Methods Appl. Mech. Eng.* **17** 419–44

Petchsuk A, Supmak W and Thanaboonsombut A 2011 Effects of size of spray-dried PZT powder and dipole density of polymer matrix on the electrical properties of PZT/odd–odd nylons 0–3 composites *J. Am. Ceram. Soc.* **94** 2126–34

Piazza D, Galassi C, Barzegar A and Damjanovic D 2010 Dielectric and piezoelectric properties of PZT ceramics with anisotropic porosity *J. Electroceram.* **24** 170–6

Ponte Castañeda P 1992 Bounds and estimates for the properties of nonlinear heterogeneous systems *Phil. Trans. R. Soc. Lond.* A **340** 531–67

Ponte Castañeda P and Willis J R 1988 On the overall properties of nonlinearly viscous composites *Proc. R. Soc. Lond.* A **416** 217–44

Rice J 1971 Inelastic constitutive relations for solids: an internal-variable theory and its application to metal plasticity *J. Mech. Phys. Solids* **19** 433–55

Sachs G 1928 Zur Ableitung einer Fleissbedingun *Z. Ver. Dtsch. Ing.* **72** 734–6

Saff E B and Kuijlaars A B J 1997 Distributing many points on a sphere *Math. Intelligencer* **19** 5–11

Smyshlyaev V and Willis J R 1998 A 'non-local' variational approach to the elastic energy minimization of martensitic polycrystals *Proc. R. Soc. Lond.* A **454** 1573–613

Tartar L 1990 H-measures, a new approach for studying homogenization, oscillation and concentration effects in partial differential equations *Proc. R. Soc. Edinb.* A **115** 193–230

Taylor G I 1938 Plastic strain in metals *J. Inst. Met.* **62** 307–24

Xu Y 1991 *Ferroelectric Materials and their Applications* (Amsterdam: North-Holland Elsevier Science)

Zeng T, Dong X L, Mao C L, Zhou Z Y and Yang H 2007 Effects of pore shape and porosity on the properties of porous PZT 95/5 ceramics *J. Eur. Ceram. Soc.* **27** 2025–9

Zhang W and Bhattacharya K 2005a A computational model of ferroelectric domains: I. Model formulation and domain switching *Acta Mater.* **53** 185–98

Zhang W and Bhattacharya K 2005b A computational model of ferroelectric domains: II. Grain boundaries and defect pinning *Acta Mater.* **53** 199–209

Zhang H, Yang S, Zhang B-P and Li J-F 2010 Electrical properties of Ni-particle-dispersed alkaline niobate composites sintered in a protective atmosphere *Mater. Chem. Phys.* **122** 237–40

Zhou D, Kamlah M and Munz D 2001 Rate dependence of soft PZT ceramics under electric field loading *Proc. SPIE* **4333** 64–70